

Uplink Throughput Performance in OFDM Wireless Systems Using Spatial Filtering of Smart Antennas

Takashi Wakutsu, Mutsumu Serizawa, Hiroki Shoki and Yasuo Suzuki
Mobile Communication Lab., R & D Center, Toshiba Corporation
1, Komukai-toshiba-cho, Saiwai-ku, Kawasaki, 212-8582, Japan
E-mail : takashi.wakutsu@toshiba.co.jp

1 Introduction

Orthogonal Frequency Division Multiplexing (OFDM) [1] systems are attracting much attention on account of their possibilities for a new business chance of broadband data distribution services. The main advantage of OFDM modulation is the characteristics to multi-path interference. In order to decide the common physical layer standard of OFDM next-generation wireless systems, a strong alignment has been achieved among three standards, IEEE801.11 (U.S), ETSI BRAN (Europe) and MMAC (Japan) [2]. These systems will support data rates up to 54 Mb/s. To provide a broadband transmission service, however, wide spectra, which are a limited resource, are needed. Therefore, efficient frequency utilization is required. The spatial filtering is one of the important solutions. As for overall system capacities, an adaptive modulation scheme [3] in which transmission rate is determined by traffic in surrounding cells is also a sophisticated approach. Since the spatial filtering of smart antennas suppresses the co-channel interference [4], a combination of spatial filtering and adaptive transmitting rate control becomes effective in terms of frequency utilization. Considering cost and size limitations, deployment of the smart antenna technologies not on a mobile terminal (MT) but on an access point (AP), which is a base station (BS), is the most reasonable scenario.

In this paper, we investigate the throughput performance in the cellular structure of OFDM next-generation wireless systems using smart antennas. We focus on the uplink carrier-to-interference plus noise ratio (CINR). The performance improvement achieved by the combination of spatial filtering and transmission rate control is demonstrated by computer simulations. Also discussed is the effect caused when the position of an interfering source changes corresponding to dynamically changing slot length and the effect of transmission power saving of a MT corresponding to the beam forming gain of a BS.

2 System model

The OFDM next-generation wireless systems have possibilities for broadband transmission. In Japan, four 5.2 GHz frequency bands (5.17, 5.19, 5.21, 5.23 GHz) will be assigned to OFDM systems. Therefore, to realize the cellular system structure, operation under severe frequency reuse is inevitable. Figure 1 shows an example of the MAC frame format. The frame is based on TDMA-TDD, and consists mainly of four sub-frames, namely BCH (for signalling message, frame information and acknowledgement to the individual MTs), uplink and downlink UCH (for user data, resource request and ARQ message), and RCH (for connection request message). The assignment of user data slot position, which is informed by FCH, is renewed at every frame. The length of each sub-frame varies according to the number of slots. Therefore, instantaneous co-channel interference changes at every moment even though the synchronization between BSs is achieved. In addition, multi-rate transmission is supported in these OFDM system standards. Table 1 shows the supporting rates [5]. The transmission rate is determined according to the

modulation level and the code rate, with consideration of wireless channel conditions. The co-channel and adjacent channel interference power depend on the number of simultaneous transmission users and the user positions. In an ordinary TDMA (or FDMA) cellular system, the distance to interfering sources depends on the reuse distance. Therefore, in the severe frequency reuse condition, introduction of spatial filtering is effective for improvement of CINR. In this investigation, we focus on the uplink CINR, and we assume that the received signal experiences path loss, and Rayleigh- and log-normal fading. The received signal power of j -th user at the target BS can be expressed by $g_j = P_j \cdot Kr_j^{-\eta} \cdot \alpha_j^2 \cdot 10^{\xi/10} \cdot I_j(\theta) \cdot B(\theta) \cdot G_b$. Here, P_j is the transmission power, $Kr_j^{-\eta}$ is the path loss, r_j is distance, α is the Rayleigh random variable, $10^{\xi/10}$ is the shadowing component, and ξ is the decibel attenuation. $B(\theta)$ and $I_j(\theta)$ are the relative radiation patterns of the target BS and the antenna of the j -th user, respectively ($\max_{\theta}[B(\theta)] = \max_{\theta}[I_j(\theta)] = 1$). G_b is the beam forming gain of the BS under receiving operation. Let us denote the input vector of each antenna element by \mathbf{X} and denote weight vector by \mathbf{W} . Then the minimum mean square error (MMSE) weight vector is calculated by $\mathbf{W} = \mathbf{R}_{\mathbf{xx}}^{-1} \cdot \mathbf{v}$. Here, $\mathbf{R}_{\mathbf{xx}} = \mathbb{E}\{\mathbf{X}\mathbf{X}^H\}$ is the correlation matrix of input vector \mathbf{X} , and \mathbf{v} is the correlation vector between the input vector \mathbf{X} and reference vector \mathbf{d} . The interference power can be described as $P_I = \sum_j g_j$.

3 Simulation results

Firstly, the average transmission rate performance against the CINR is evaluated. The results are shown in Fig. 2. Major parameters are shown in table 2. In this simulation, the interference was assumed an additional AWGN. The 3/4 code rate can be obtained by puncturing the original coded bits of rate 1/2 [6]. The rate 9/16 is made by puncturing 2 out of every 18 coded bits. If an optimal link adaptation based on channel conditions is employed, an appropriate pair of the modulation and the code rate is selected, the best throughput performance corresponding to the top curves illustrated in Fig. 2 can be achieved [7].

Next, we evaluate the probability density performance of CINR. We assume an ordinary hexagonal cell allocation. The number of reuse frequency bands is 3 and 4. Figure 3 shows examples of the frequency reuse of a hexagonal cellular structure. The distance between cell centers is $3R$ (three frequency reuse) or $2\sqrt{3}R$ (four frequency reuse). In this investigation, the cell radius is set to $R = 80$ m. A MT position is randomly chosen within a cell area by using a uniformly distributed random number. The path loss exponent is set to $\eta_D = 2.5$ for intra-cell propagation (i.e. for desired signal) and $\eta_U = 3.0$ for inter-cell propagation (i.e., for undesired signal), respectively. The standard deviation of the log-normal fading loss is set to 8.5 dB. Further, 2 tire co-channel interference is considered, that is, the number of co-channel interference signals is 6. The upper and lower adjacent channel interferences are also considered, and the adjacent channel suppression level is set to 25 dB. The system load of each cell is set to 100%, and the ratio of uplink and downlink slots is set to 0.5. The transmission power is 20 dBm, and noise power is -93 dBm. Moreover, the number of antenna elements of the BS is set to $L = 4, 8$. Each element is an omnidirectional antenna and the antenna elements were arranged in a circle. The spacing distance was set to $\lambda/2$, where λ is the wavelength. The MT antenna is assumed to be omnidirectional. Furthermore, we assume that the pilot of the desired signal is non-coherent with the other undesired signals.

Figure 4 shows an example of a relative radiation pattern (In this figure, the CINR was equal to 25 dB). The time-domain signals of a pilot symbol were used for the antenna weight calculation (The number of pilot samples is 128). In the OFDM systems in which a user data slot length is dynamically changing, the beam pattern that has been determined once may not be effective because the direction of arrival (DOA) of interfering signals changes. Therefore, null-steering of smart antennas is not effective even though the degree of freedom for null-

steering is large enough. Moreover, in the OFDM systems, the transmission power is specified by EIRP. Therefore, for the downlink, we cannot expect the improvement of CNR corresponding to the beam forming gain because deployment of smart antenna technologies on MTs is not an appropriate scenario. However, the beam forming to the desired user brings the effect of spatial filtering that is superior to suppression of average interference power. In addition, the beam forming gain of the target BS makes it possible to save the transmission power of a MT since the beam forming gain improves the CNR at the target BS. In this investigation, in order to make the radio link quality identical to that of the downlink, we employ the MT transmission power saving (TPS) corresponding to the beam forming gain of the BS. The beam forming gain changes according to a beam pattern, and we set the saving power to 4.9 dB for $L = 4$, and 7.5 dB for $L = 8$, which are mean values. The MT TPS can relieve the specification for a power amplifier of a MT.

Figure 5 shows the cumulative probability density (CPD) of CINR. The CPD is obtained by 10000 times trials. $L = 1$ means the condition without (w/o) beam forming (i.e., $B(\theta) = 1 \forall \theta$). For the $L = 1$ and four frequency reuse case, $\text{CINR} > 6$ dB is achieved in the area of 95% of the whole area. If $\text{CINR} > 6$ dB, the modulation no less than QPSK can be applied (Fig. 2). In other words, in order to provide the transmission rate no less than 12 Mb/s (QPSK, rate=1/2) for the area of 95 %, four frequency reuse or the smart antenna technology is required. By introduction of smart antennas, the required CINR is improved by about 4 dB.

Finally, we evaluate the throughput performance of the OFDM cellular systems. The results are shown in table 3. Here, ideal selection of an appropriate transmission rate was assumed. From table 3, the throughput performance no less than 20 Mb/s can be achieved with the $L = 1$, three frequency reuse condition. When spatial filtering of smart antennas and MT TPS are introduced, throughput performance is improved by about 5 Mb/s compared with the result over w/o beam forming condition. This improvement can be attributed to the interference suppression by spatial filtering, since the improvement due to the beam forming gain is compensated by TPS. Moreover, comparing the result with the $L = 1$, w/o other cells and the results with $L = 4, 8$, frequency reuse condition, we found that the average interference power is suppressed adequately by spatial filtering of smart antennas.

4 Conclusions

In this paper, the uplink throughput performance in the cellular OFDM systems has been investigated. The cumulative probability distribution of the CINR has been evaluated as a function of the number of antenna elements, MT transmission power saving, and reuse distance. The performance improvement under severe frequency reuse conditions has been confirmed. The investigation over more realistic propagation parameters is planned as a future work.

References

- [1] L. J. Cimini Jr., "Analysis and Simulation of a Digital Mobile Channel Using Orthogonal Frequency Division Multiplexing," *IEEE Trans. Commun.*, vol.COM-33, No.7, pp.665–675, July 1985.
- [2] MMAC Wireless Access Specification Version 1.1, Nov. 1999.
- [3] S. Sampei et al., "Adaptive Modulation/TDMA Scheme for Large Capacity Personal Multi-Media Communication Systems," *IEICE Trans. Commun.*, vol. E77-B, no.9, pp.1095–1103, Sept. 1994.
- [4] T. Ohgane, "Spectral Efficiency Improvement by Base Station Antenna Pattern Control for Land Mobile Cellular Systems," *IEICE Trans. Commun.*, vol. E77-B, no.5, pp.598–605, May 1994.
- [5] J. Torsner et al., "Radio Network Solutions for HIPERLAN/2," *Proc. IEEE VTC'99 Spring*, pp.1217–1221.
- [6] D. Haccoun et al., "High-Rate Punctured Convolutional Codes for Viterbi and Sequential Decoding," *IEEE Trans. Commun.*, vol.36, pp.1113–1125, Nov. 1989.
- [7] S. Muneta et al., "A New Frequency-domain Link Adaptation Scheme for Broadband OFDM Systems," *Proc. IEEE VTC'99 fall*, pp.253–257.

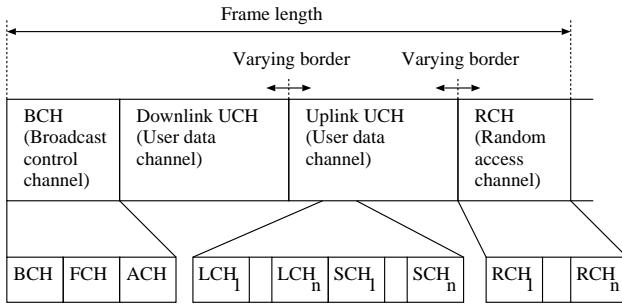


Fig. 1 MAC frame format.

Table 1 Supporting data rates.

Data rate	Modulation	Code rate
6 Mb/s	BPSK	1/2
9 Mb/s	BPSK	3/4
12 Mb/s	QPSK	1/2
18 Mb/s	QPSK	3/4
27 Mb/s	16QAM	9/16
36 Mb/s	16QAM	3/4
54 Mb/s	64QAM	3/4

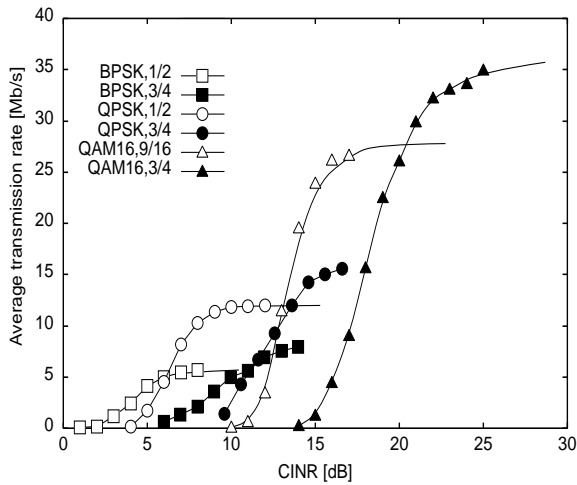
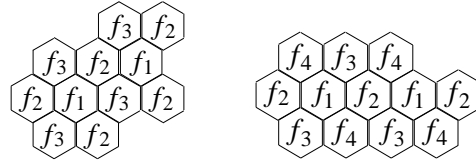


Fig. 2 Average transmission rate performance against CINR.

Table 2 Parameters.

Sub-carrier frequency spacing	312.5 kHz
Guard interval	0.8 μ sec (1/4)
Number of data sub-carriers	48
FEC	Convolutional encoding, Viterbi decoding (K=7)
Interleaving	OFDM-symbol period
Rms delay spread of multipath channel	100 nsec
Data length	64 bytes
ARQ	Ideal selective repeat



(a) 3 frequency reuse (b) 4 frequency reuse
Fig. 3 Frequency reuse of a hexagonal cellular structure.

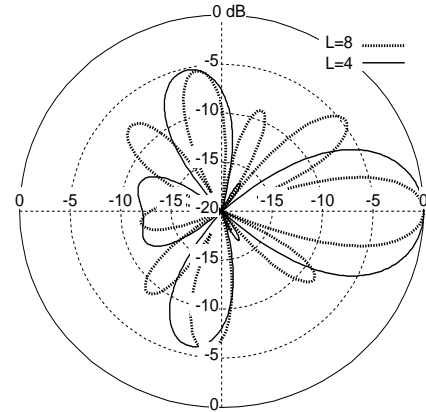


Fig. 4 An example of relative radiation pattern.

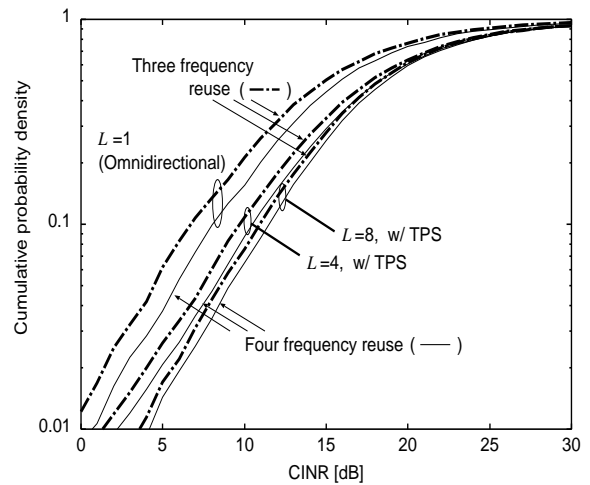


Fig. 5 Cumulative probability density of CINR.

Table 3 Throughput performance.

Conditions	Throughput [Mb/s]		
	Number of reuse frequencies		w/o other cells
	3	4	
$L = 4$ (w/o TPS)	27.9	29.0	32.1
$L = 8$ (w/o TPS)	30.5	31.4	33.7
$L = 1$	21.1	22.6	27.5
$L = 4$ (w/ TPS)	25.0	25.5	27.5
$L = 8$ (w/ TPS)	25.9	26.4	27.5